LAWRENCE
LIVERMORE
NATIONAL
LABORATORY

LLNL-CONF-718297

Broadband laser ranging development at the DOE labs

C. V. Bennett, B. M. La Lone, P. W. Younk, E. P. Daykin, M. A. Rhodes

January 18, 2017

SPIE Photonics West 2017
San Francisco, CA, United States
January 28, 2017 through February 2, 2017

Disclaimer

This document was prepared as an account of work sponsored by an agency of the United States government. Neither the United States government nor Lawrence Livermore National Security, LLC, nor any of their employees makes any warranty, expressed or implied, or assumes any legal liability or responsibility for the accuracy, completeness, or usefulness of any information, apparatus, product, or process disclosed, or represents that its use would not infringe privately owned rights. Reference herein to any specific commercial product, process, or service by trade name, trademark, manufacturer, or otherwise does not necessarily constitute or imply its endorsement, recommendation, or favoring by the United States government or Lawrence Livermore National Security, LLC. The views and opinions of authors expressed herein do not necessarily state or reflect those of the United States government or Lawrence Livermore National Security, LLC, and shall not be used for advertising or product endorsement purposes.

Broadband laser ranging development at the DOE labs

Corey V. Bennett*[a], Brandon M. La Lone[b], Patrick W. Younk[c], Ed P. Daykin[d], Michelle A. Rhodes[a]
[a]Lawrence Livermore National Laboratory, P.O. Box 808, L-186, Livermore, CA USA 94551;
[b]National Security Technologies, LLC, Special Technologies Laboratory, Santa Barbara, CA USA 93111; [c]Los Alamos National Laboratory, Bikini Atoll Rd., SM 30 Los Alamos, NM USA 87545;
[d]National Security Technologies, LLC, P.O. Box 98521, NLV-073, North Las Vegas, NV USA 89193-8521

ABSTRACT

Broadband Laser Ranging (BLR) is a new diagnostic being developed in collaboration across multiple USA Dept. of Energy (DOE) facilities. Its purpose is to measure the precise position of surfaces and particle clouds moving at speeds of a few kilometers per second. The diagnostic uses spectral interferometry to encode distance into a modulation in the spectrum of pulses from a mode-locked fiber laser and uses a dispersive Fourier transformation to map the spectral modulation into time. This combination enables recording of range information in the time domain on a fast oscilloscope every 25-80 ns. Discussed here are some of the hardware design issues, system tradeoffs, calibration issues, and experimental results. BLR is being developed as an add-on to conventional Photonic Doppler Velocimetry (PDV) systems because PDV often yields incomplete information when lateral velocity components are present, or when there are drop-outs in the signal amplitude. In these cases, integration of the velocity from PDV can give incorrect displacement results. Experiments are now regularly fielded with over 100 channels of PDV, and BLR is being developed in a modular way to enable high channel counts of BLR and PDV recorded from the same probes pointed at the same target location. In this way instruments, will independently record surface velocity and distance information along the exact same path.

Keywords: Optical Ranging, Ultrafast ranging lidar, LIDAR, Interferometry, Dispersive Fourier transform, Remote sensing and sensors, Ultrafast technology, Laser range finder

1. INTRODUCTION

1.1 Our applications

The DOE national security labs, as part of their stockpile stewardship mission and in support of missions for many other government agencies, regularly perform explosively driven experiments to study shock physics, material flow, energetics, safety, systems performance, and etc. at a variety of scales. These experiments and the various facilities in which they are preformed present a dramatic range in operating and environmental conditions within which we must make precision measurements of surfaces and materials moving at speeds from around 1 km/s to nearly 10 km/s. We often wish to track surfaces over more than a 10 cm range of travel, and require well under 100 μm maximum error in measured position. There may be 10s to well over 100 individual position measurement channels which must all be cross timed to less than 1 ns in order to track a three-dimensional surface.

Small experiments are performed in a typical laboratory environment using steel containment vessels. Larger experiments can be performed in bunkers, such as the Contained Firing Facility (CFF) at LLNL which can detonate up to 132 lbs of high explosives (HE) in a 50 ft x 50 ft x 30 ft bunker made of 6 ft thick reinforced concrete walls. Even larger experiments can be performed at outdoor firing facilities. If the experiment is too hazardous, it can be performed nearly 1000 ft underground at the Nevada National Security Site (NNSS). The facilities are large complex environments, with containment vessels to withstand explosive forces and hold back hazardous materials. We must make precision, high speed, and broad bandwidth measurements inside this environment while protecting valuable equipment and people outside. It is thus advantageous to have cheap, disposable sensing elements near the explosion that send signals through optical fiber to the costly recording elements in remote diagnostic chambers. Broadband Laser Ranging (BLR) is being pursed as a position measurement diagnostic that meets these needs and conforms well to the challenges of this experimental environment.

*CVBennett@LLNL.gov; phone 1 925 422-9394; www.LLNL.gov

1.2 Limitations of existing technologies for measuring position

Experiments for these applications performed years ago, often used pins. Each pin measures the arrival time of a surface at a single point in space. Many pins were required to get the position vs. time of an approaching point on a surface, and many more pins were required to get a surface profile vs. time. "Pin domes" have many pins of different lengths pointing in many different directions. Experiments with such measurement tools are extremely difficult and time consuming to build and calibrate. In contrast, optical reflection based measurement utilizing one probe (lensed fiber) can record the entire travel of a surface along the path of the laser beam, and optical probe domes are compact and easier to calibrate.

Photonic Doppler Velocimetry (PDV) has been developed to measure the velocity of a surface along a projected laser beam[1,2]. A very narrow band cw laser is used to illuminate a target, as well as to mix with Doppler shifted light reflected from the surface. The beat frequency between the signal and reference changes with velocity and can be analyzed to give a velocity vs. time profile of the surface moving along the beam. The biggest issue with PDV is that integrating the measured velocity does not always produce a correct position vs. time. Most notably, PDV only measures the velocity component in line with the beam and provides no information of possible orthogonal surface flow[3]. It's also common for optical-based measurements to have periods of low or no signal due to speckle and surface deformation effects or debris in the beam. If velocity data is missing for any part of the record, then the position for all times afterward is uncertain. When shock fronts break out of a surface, and at other moments of extreme accelerations, measured velocities are not always accurate enough. There are many cases in which one cannot integrate a PDV measurement to get an accurate position vs. time. Another technology was needed that truly measured position.

1.3 Broadband Laser Ranging introduction

Early work demonstrating this ranging technique was performed by Xia and Zhang[4,5] and came to the attention of La Lone, Marshall, et.al. at National Securities Technologies (NSTec), who demonstrated the value of this diagnostic to DOE applications. They extended the range to 4.4 cm, improved the sensitivity, and combined it with a PDV measurement on the same probe[6]. They also coined the name Broadband Laser Ranging (BLR), which has stuck within the DOE complex. La Lone presented this work at LLNL in Nov. 2014 and by May 2015 we had demonstrated a system utilizing larger dispersion modules and distributed Raman amplification to produce a system with 12 cm target tracking utilizing a 14 GHz detection bandwidth[7]. Two channels of a slightly improved version of this single-channel architecture were deployed on an important experiment at LLNL's CFF in Dec. 2015 and will be discussed more here. Today many within the DOE are collaborating on the development of a modular multiplexed BLR systems which can easily scale up to the large channel counts.

Let's first discuss the operation of a single channel system. Idealistic frequency vs. time diagrams out of the interferometer, and after dispersion, are shown in Figure 1 for a system shown in Figure 2. BLR uses an interferometer to modulate the spectrum of a mode-locked laser pulse train. In the idealized case where the two branches of the interferometer are matched in chromatic dispersion and differ only in time delay $\Delta\tau$, the interference in the spectral domain will oscillate in intensity constructively and destructively with a periodicity, or Free Spectral Range (FSR),

$$\Delta\upsilon_{FSR} = 1/\Delta\tau \,. \tag{1}$$

The interferometer output is followed by amplified dispersive Fourier transformation[8] to map the spectrum of the pulses into time at a scale slow enough to resolve this spectral modulation in the time domain. In an idealized system where the pulses are chirp free, or Fourier Transform limited, on target and the fiber optic system performing the dispersive Fourier transformation has perfectly linear chromatic dispersion, the change in delay with optical frequency is

$$\frac{d\tau}{d\upsilon} = 2\pi L\beta^{(2)}, \tag{2}$$

where L is the length of the dispersive fiber and $\beta^{(2)}$ is its group velocity dispersion, or second derivative of the propagation constant, described further below. Ideally the pulses in time would look just like their spectral counterparts, with the mapping to time enabling the spectrum to recorded at high repetition rates (>10^7 measurements/sec) over long records (>100 μs) using modern oscilloscopes. Each pulse or measurement frame would contain a beat frequency F recorded at the final output photoreceiver and digitizer

$$F = 1 \Big/ \left(\upsilon_{FRS} \cdot \frac{d\tau}{d\upsilon} \right), \tag{3}$$

Assuming the difference in position from the balance point of the interferometer Δd is double passed on reflection from the target, the distance in an ideal system is calculated as

$$\Delta d = \frac{c/n}{2\,\Delta\upsilon_{FSR}} = \frac{(c/n)F}{2}\frac{d\tau}{d\upsilon} = (c/n)F\pi L\beta^{(2)}. \tag{4}$$

An idealized frequency vs. time representation of the reference and signal pulses returning from the interferometer and after being dispersed and detected by the photoreciever is shown in Figure 1. The figure represents one measurement and happens repeatedly at the repetition rate of the laser. At the left are two compressed pulses returning from the target and reference respectively. After being dispersed linearly there is a constant offset frequency between the signals causing a constant beat frequency F in time determined by the time delay $\Delta\tau$.

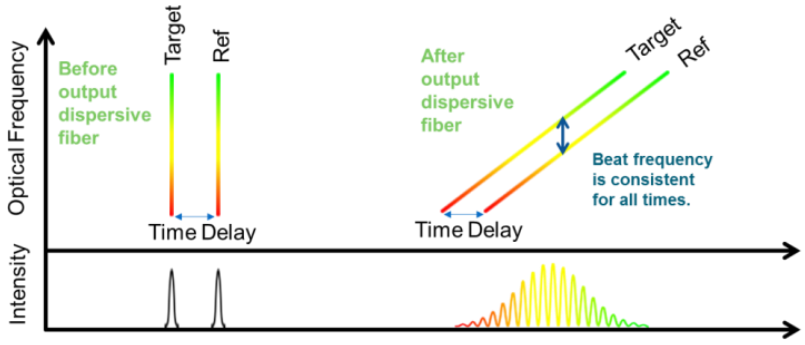

Figure 1. An idealized frequency vs. time diagram showing pulses of differing delay from the target and reference being dispersed and beating at the output of the system.

A simplified conceptual diagram of the systems utilized at LLNL's Contained Firing Facility (CFF) in Dec. 2015 is shown in Figure 2. Standard PDV was multiplexed onto the target at the same target location utilizing a CWDM filter with PDV in the 1550 nm band and BLR in a 15 nm band at 1570 nm. The laser source was a Menlo Systems 100 MHz mode-locked laser pulse picked down to 12.5 MHz. A fiber circulator sent the laser source pulse train to the experiment inside the CFF chamber approximately 30 m from the instruments. The source pulses were split into two legs of a Michaelson interferometers utilizing a 75%/25% splitter with short matched fiber lengths and filters so that the chromatic dispersion of each leg was nearly identical. Fiber optic collimator probes were used to illuminate the target in the signal (75%) leg with around a -55 dB return, and a fixed high reflective reference mirror in the reference (25%) leg positioned approximately mid-way in the expected delay range of the target.

The return light has a strong pulse envelope determined by the reference leg, but with a spectral modulation introduced by the interference with the moving signal returning from the HE driven target. The returning spectrum was dispersed and amplified in a "200 km" Dispersion Compensation Module using OFS dispersion compensation fiber designed to have chromatic dispersion opposite of that of 200 km of SMF-28, or approximately -3.6 ns/nm. The DCM module had around 11 dB of loss but was converted into a distributed Raman amplifier by pumping it backwards with light near 1465 nm. Up to 30 dB of Raman gain was available with approximately 400 mW of pump power, and 20 dB of gain was used for the experiment. Miteq SCMR-100K20G photorecievers and a Tektronix DPO72004B oscilloscope recorded the final signals with 20 GHz bandwidth at 50 Gsample/sec.

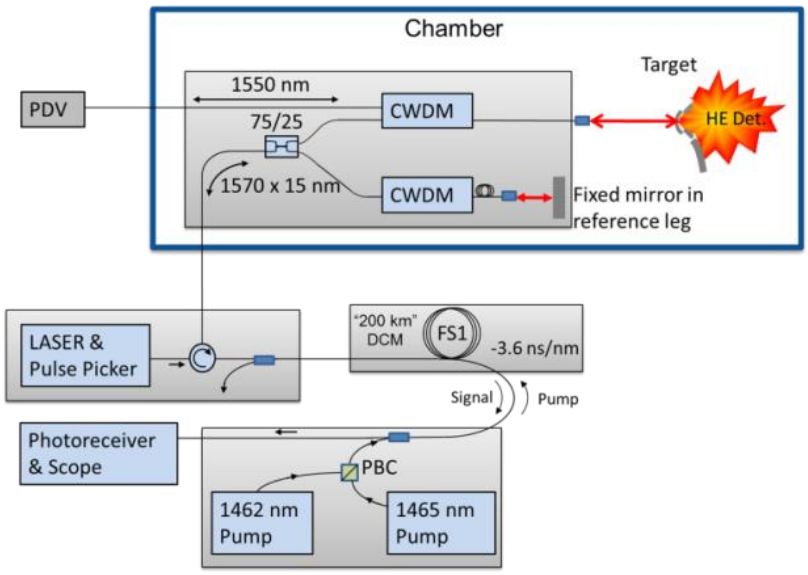

Figure 2. Cartoon of first generation prototype BLR system fielded at CFF in Dec. 2015.

Data analysis for BLR systems is discussed in detail in the next paper of this session[9]. In summary, it involves parsing out and registering the separate pulses in the scope record into frames. Two pulses (out of many thousands) are shown in Figure 3 below. Here spectral filters with sharp filter edges were intentionally included in the system to provide clear spectral reference points for registering frames from the many individual measurements. A smoothed envelope of the frames must be found and subtracted to obtain the modulation detail in blue. Time and frequency domain corrections may be applied to correct for effects described in Section. 2. Each frame is then Fourier transformed to give the spectrum or beat frequency of that frame. The spectrum scaled to space using (4) or a calibration measurement, producing the middle plot in Figure 3. In the simple case of a single moving surface a peak extraction algorithm gives the position vs. time information shown on the right of Figure 3. BLR gives precise information about the change in position relative to the starting location and the balance point location as a function of time, but due to the sensitive nature of this particular experiment, the data has been normalized for publication. Features clearly observable in this data is the initial position and time of first motion in the upper left of spectrogram and extraction, as well as the acceleration of the surface as it approaches the probe. The blue to yellow color scale in the spectrogram and extraction represents the magnitude of the FFT peak and scales a 30 dB range.

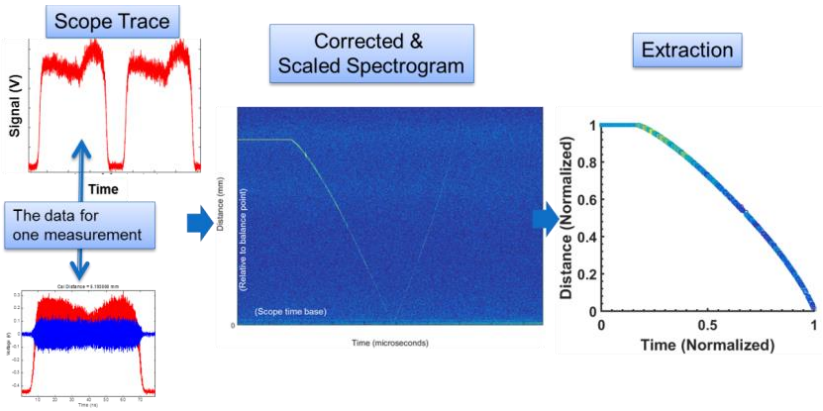

Figure 3. Example data analysis process. Left: Two frames from the raw record on the left, with one parsed and envelope removed frame below. Center: Plot of scaled spectrogram found by Fourier Transforming each frame. Right: Extracted position vs. time from peak tracking in spectrogram. BLR gives real distance and time, but data is normalized here.

2. HARDWARE ISSUES & NON-IDEALITIES

The previous discussion presented an idealized concept of operation and description of an example real system. In reality few subsystems are ideal. It's also possible to compromise some performance issues to improve the overall system performance. Below discusses practical hardware issues and the tradeoffs.

2.1 Doppler Effect

Light of frequency υ retro reflected from a high velocity moving target with velocity V will be Doppler upshifted $\Delta\upsilon_D$ as given by

$$\frac{\Delta\upsilon_D}{\upsilon} = \frac{2V}{c/n}, \tag{5}$$

where c/n is the speed of light in the gas in which the reflective surface is moving. If the optical pulse on target is chirp free, as in Figure 1, the returned light off the target will be shifted up in frequency in the left part of Figure 1, and shifted along the dispersed target line in the right side of the diagram. The separation between the two dispersed spectra, and thus recorded beat frequency, is unchanged. Ideally BLR systems are immune to the Doppler Effect, but it can be difficult to deliver pulses that are exactly chirp free on target. In addition, it is often advantageous from a peak power handling perspective to avoid compressing the pulses fully.

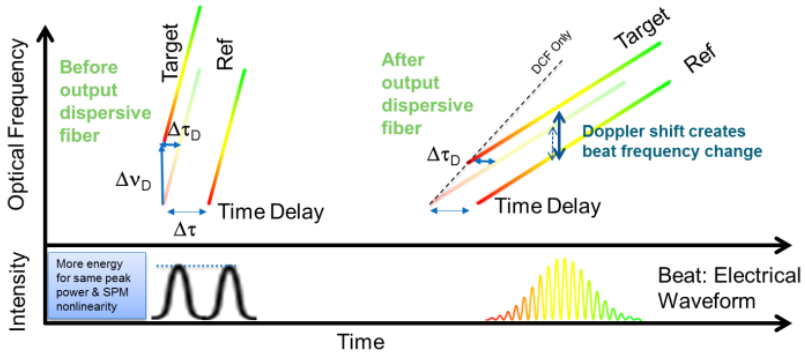

Figure 4. Idealized frequency vs. time plots of a BLR system including chirp on target and a Doppler shift of the light returning from a fast moving target.

If the pulses are chirped on target, as shown in Figure 4, they will experience the same Doppler upshift $\Delta\upsilon_D$, but also experience a slight effective time shift

$$\Delta\tau_D \approx \frac{\Delta\upsilon_D}{(d\upsilon/d\tau)} = \frac{2n\upsilon V}{c(d\upsilon/d\tau)} \tag{6}$$

after propagation through the output dispersion. This is in addition (depending on sign of chirp) to the real target motion in (1). Expressing the chirp on target in terms of an equivalent length L_{equiv} of SMF-28 fiber propagation from the point of transform limit, one can derive a useful expression for the Doppler displacement error,

$$\begin{aligned} \Delta d_D &= \left(2\pi\upsilon\beta^{(2)}\right) L_{equiv} V \\ &\approx \left(-28\mu m/km/(km/s)\right) L_{equiv} V \end{aligned} \tag{7}$$

with the constants evaluated at the long wavelength end of the telecom C-band where mode locked fiber laser sources are abundant. Multiple BLR systems are being designed. In some systems this effect is designed to be small enough at velocities of interest as to be insignificant to the overall error budget. In others, correction is necessary. Correction requires precision knowledge of the chirp on target $d\upsilon/d\tau$ and either an independent synchronized velocity

measurement or extraction of a velocity estimate from the slightly erroneous position profile. An estimated velocity dependent position error can then be subtracted to produce a position vs. time profile with a reduced and acceptable error. This approach is currently under development for certain applications.

2.2 Losses and signal to noise

A fundamental difficulty is maintaining good signal-to-noise ratio (SNR) in these systems is that they inherently have high losses. The need for broad bandwidth propagation and a stable phase for interferometry necessitate propagation of our signals on single mode optical fiber. A lensed fiber, or probe, is used to illuminate a spot on the surface of our explosively driven surface. If the surface was specular and accidentally titled from normal to the incent beam, all return power could be lost. Surfaces are thus usually rough and diffuse, creating a noisy speckle pattern with substantial loss and power variation when coupling back into a single mode fiber. Optical returns of -55 dB or less are typical.

There are many dynamic affects in these experiments which can have even weaker returns than the pre-shot surfaces. Ejecta clouds, jetting of material, surface blistering and scabs, debris in the beam path, and the surface melting or vaporization are all common dynamic effects we wish to see with this diagnostic. These features can be very small, reflecting only part of the energy back, or large and reflect much of the energy back or out of the beam. Return levels are very dynamic and we regularly pull important information out of spectrograms over more than 30 dB dynamic range. Further improving this dynamic range would be very beneficial and is an area of current research.

Another fundamental challenge is the loss in the dispersion compensation fiber (DCF) or module (DCM) used to map spectrum into time. These instruments need very large dispersions on the order 1 to 4 ns/nm depending on the range desired and bandwidth of detection electronics. DCMs in the range of “60 km” to “200 km” have been used and are so named because they compensate for this length of standard SMF-28 fiber, but are nearly 10x shorter, saving space and reducing signal delay and cross timing problems. These DCMs often have more than 10 dB loss.

For these instruments to have no velocity (Doppler) dependent error, pulses should be Fourier transform limited, or chirp free, on target as discussed above. But high peak powers can drive self-phase modulation (SPM) nonlinearities in the fiber and distort our signals. This limits the energy per pulse before the target and makes it difficult to overcome losses later in the system by simply turning up the source laser power.

Two different approaches to dealing with this trade-off between Doppler induced error and SNR are being investigated within the DOE. At LLNL a system is being designed in which the chirp on target is small enough that the Doppler induced error is a small part of an overall error budget and can thus be ignored in the data analysis. Pulses with a 19 nm bandwidth, which would be around 170 fs in duration if optimally compressed, are instead chirped to 37 ps duration on target and start experiencing SPM effects at energies around 0.2 - 0.5 nJ/pulse. This threshold was determined by estimating the pulse duration along the fiber from the laser source to the target and finding the energy at which the peak nonlinear induced phase change is around 1 radian.

$$\phi_{Pk-NL} = \int \frac{2\pi n_2}{\lambda A_{eff}} \frac{E}{\Delta t(x)}\, dx \approx 1 \tag{8}$$

The chirp mentioned above is equivalent to 110 m of SMF-28 fiber length needed to remove it. At a nominal velocity of 5 km/s, a Doppler error of 15 μm is expected. This is acceptable without correction but the limited source energy at the front end make high quality back end amplification even more critical.

Recognizing the Doppler Effect as well understood physics, LANL has placed SNR as the first priority and plans to correct the induced Doppler error in numeric post processing. They’re designing a system capable of putting more energy on target and experimenting with configurations having approximately an order of magnitude more chirp on target, with the same bandwidth. Pulse durations are several hundred ps on target and allow for several nJ/pulse to be delivered with negligible nonlinearity. For the same speed of 5 km/s this system produces a 150 μm offset in measured position, which is too large to be ignored. The analysis code must extract an initial estimate of the position vs. time, determine the approximate velocity, and apply a correction to the position. The analysis approach is still under development but for clearly identifiable surfaces it appears to be working well. Doppler correction in the presence of jets, ejecta, and debris may be more difficult.

LANL experiments also tend to indicate that BLR can be more robust to SPM than (8) would suggest. They have driven well above this limit and obtained reasonable range measurements, but detailed error analysis is still ongoing.

2.3 Unmatched interferometer legs

In general, the delay of any given fiber optic component in the system is a function of its chromatic dispersion characteristic and the exact wavelength it is measured. At the balance point of the BLR interferometer the total group delay of the signal leg must match that of the reference leg over the spectrum being measured or instead of a single position mapping to a single delay, it will map to a range of delay and blur our signal. An interferometer with imbalanced dispersion characteristics creates a chirp in the free spectral range about the nominal frequency associated to the real position and lowers the resolution of the system.

If the legs of interferometer are short, on the order of meters, this issue is easily negligible. But that can require splitter, time delay, and polarization control optical components to be placed in a hazardous environment where they will be destroyed on every shot and where human access to these components is limited. Operationally it is advantageous to have long interferometer arms with adjustable components safely back in the diagnostic room, in some facilities up to 200 m away from the experiment.

From typical Corning SMF-28 fiber specifications, a 10% change in the dispersion D [ps/nm/km] is possible from one lot to another. Looking at the difference in sums of fiber lengths L and dispersions D over the signal and reference legs of the interferometer, a variation in the roundtrip delay measured $\Delta\tau_{meas}$ over the measurement spectrum $\Delta\lambda$

$$\Delta\tau_{meas} = 2\left(\sum_{sig} LD - \sum_{ref} LD\right)\Delta\lambda \tag{9}$$

causing and apparent distance blur

$$\Delta d_{meas} = c\,\Delta\tau_{meas}/(2n). \tag{10}$$

For long interferometers it's possible for this blurring to be on the scale of a mm if nothing is done about it.

The effect is not easily corrected numerically with a simple scaling of the raw data as it depends on the position of the surface and there may be multiple surface, ejecta, etc. at different distances in a record of interest. There has been some investigation of correcting this effect with wavelet transforms, but we have primarily chosen to address this problem in the hardware. We have either kept the interferometers short enough to avoid this effect, or performed sorting experiments for long interferometers to find matched pairs of fibers in the ribbon fibers where dispersion profiles were closely matched. For future high channel count experiments we are pursuing ribbon fibers where all strands of the ribbon come from one spool and thus have the same dispersion.

2.4 Third-order dispersion in output fiber

One of the first most obvious distortions from ideal experienced when building these systems is that the mapping of spectrum into time is nonlinear due to curvature in the chromatic dispersion characteristics of optical fibers. An optical fiber with propagation constant

$$\beta(\omega-\omega_0) = \sum_{n=0}^{\infty} \frac{\beta^{(n)}\cdot(\omega-\omega_0)^n}{n!} \tag{11}$$

has a group delay dispersion

$$\frac{d\tau(\omega-\omega_0)}{d\omega} = L\beta^{(2)} + L\beta^{(3)}\cdot(\omega-\omega_0) + \ldots \tag{12}$$

where L is the length of fiber. The higher order terms chirp the output dispersion, resulting in a chirped beat recorded on an oscilloscope even if the FSR is not chirped. What should be a single frequency tone becomes a chirp which increases in rate as the center frequency or range increases. It is shown conceptually in Figure 5 and discussed in detail in the following paper of this session[9]. Since the spectral components of our pulses are mapped into time, this effect can easily

be corrected for short, dispersion-balanced interferometers having a constant FSR, by scaling the time of each frame to produce one constant beat frequency.

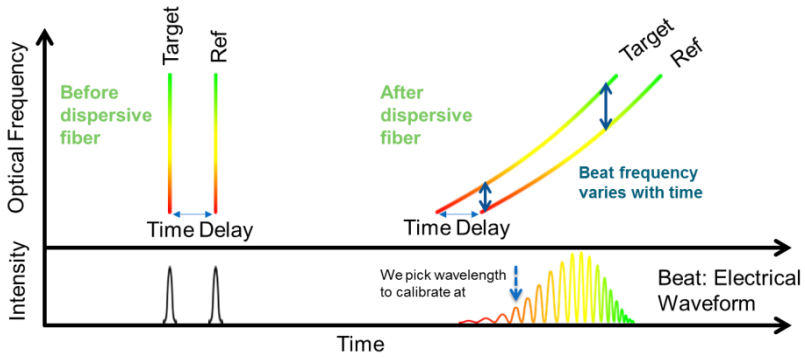

Figure 5. Frequency vs. Time plots showing the chirped beat produced by third-order dispersion of the output fiber nonlinearly mapping spectrum to time.

Early experiments used well balanced interferometers producing no other significant chirping effects. They also included filters to produce a well-defined spectral edge, acting as a fiducial to register the data in each frame (as seen in Figure 3). With every frame carefully parsed and registered the same way, parameters for (12) could be found that would produce an optimum compressed and peaked FFT of a measurement frame for a given calibration distance. Calibration data was taken a priori and the time scale correction parameters and calibration slopes were assumed to be still valid during the shot taken sometimes days later.

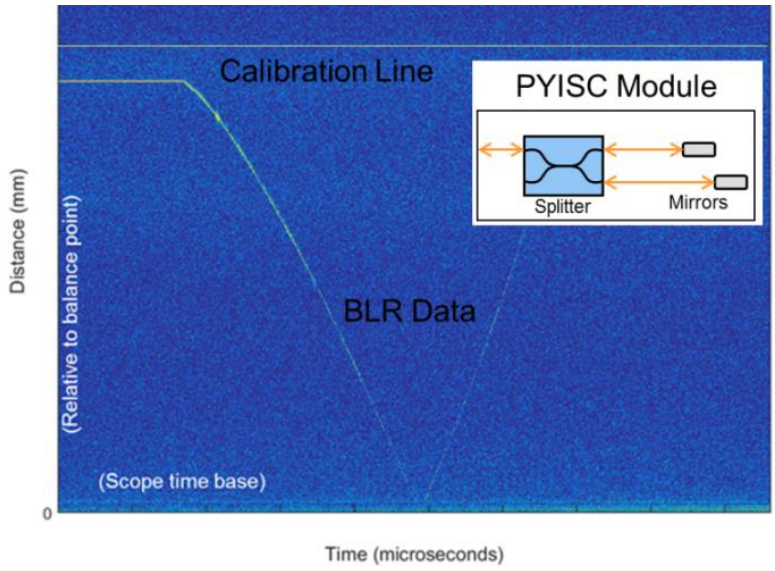

Figure 6. Patrick Younk In Situ Calibration module replacing the reference mirror creates a line in the spectrogram which can be used to simplify calibration and separate the effects of various distortions.

To simplify the calibration process the Patrick Younk In Situ Calibration (PYISC) module was proposed. Systems currently under development are replacing the reference mirror of the interferometer with another interferometer having a strong reference return from the primary mirror and a small secondary (approximately 1% of the main reference) reflection with an a priori precision-known delay difference. This creates a stable beat frequency line in the spectrograms which has this third-order output dispersion effect, providing in situ information with which it can be corrected, and is at a known stable distance with which to scale the spectrograms. Since this PYSIC module interferometer legs are short, it is inherently more stable than the main longer interferometer and allows us to separate physics of various distortions and instabilities.

2.5 Thermal variations

Experimental conditions for DOE applications vary from lab environments, to warehouse like facilities, to large concrete bunker like chambers, to open experiments in the desert, to experiments in tunnels nearly 1000 ft underground. The combination of thermally induced index of refraction change and thermal expansion changes the signal travel time in optical fibers on the order of $\Delta\tau/\tau \approx 10^{-5}/^{\circ}C$. This leads to fundamental drifts we must deal with which cause different issues depending on where in the system they are.

Fibers to and from the experiment may be 10 to 200 m in length, up to 1 μs in delay. This delay will change due to external facility environment variations, which can change with the weather. Differential delay changes of as little as 6.6 fs between interferometer legs appear as μm motions and thus it is impossible to calibrate the absolute position of a surface a priori using BLR. We count on the calibration slope being stable, not the absolution positions, and are measuring it in situ with the PYISC modules discussed above in future systems. BLR accurately measures movement from the starting location, which is independently measured before the experiments with multiple techniques.

Dispersion modules and delay lines (discussed below) with 50 to 150 μs propagation delays are part of the instrumentation racks, which also contain many kW dissipating oscilloscopes. Racks vary over $15^{\circ}C$ in some applications, making cross timing many diagnostic channels (BLR and PDV) to sub 1 ns challenging. Some facilities have integrated single mode fiber timing measurement systems which are being redesigned to work with the high dispersions of BLR systems, and a timing fiducial injection system based on single shot pulsed modulation of a narrow bandwidth laser is also under development. This fiducial system injects a pulse derived from a common trigger system before all lengthy fibers shifting with their delay changes and providing an in situ timing reference.

Chromatic dispersion of fibers can also vary with temperature[10]. An early estimate for a larger DCM indicated that a change of $10^{\circ}C$ was enough to change how the spectrum dispersed in time was sampled by the oscilloscope. In situ calibration with the PYISC modules solves this issue as well.

3. FUTURE MULTICHANNEL SYSTEMS UNDER DEVELOPMENT

There are multiple variations on a modular multichannel architecture being developed and tested, but most fit a common goal of sharing one laser source and one oscilloscope for eight BLR channels, the laser and high-speed oscilloscope being the most expensive components of the system. The systems have a common architecture but are being optimized based on facility needs, component availability, and schedules unique to various facilities. Figure 7 shows a conceptual design of the system being developed at LLNL for CFF and similar facilities. A team lead by LANL, and driven by earlier deployment schedules, has a similar 8-channel R&D system operational at NNSS.

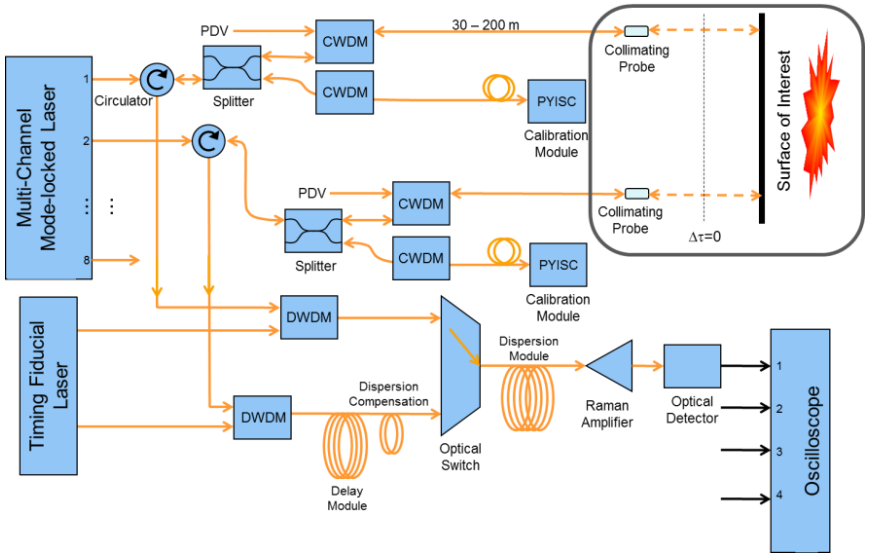

Figure 7. A conceptual design of an 8-channel system being developed at LLNL. A team lead by LANL has a similar 8-channel system operational at NNSS.

3.1 Front end multiplexing

Sharing of a common laser source is being referred to as "Front end multiplexing." Current systems under development start with a common mode locked laser oscillator either at 20 or 40 MHz. This is followed by a combination of preamplification in an EDFA and chirping either with DCF or SMF28. There is then a 1x8 splitter creating multiple outputs. Systems with small chirps have eight separate post amplifier EDFAs, whereas systems with very large prechirps can get away with a single high power preamp and experience insignificant SPM. Systems typically utilize approximately a 20 nm bandwidth centered either at 1560 nm or 1555.8nm.

3.2 Sensing Interferometer and In Situ Calibration

Pulses from the laser then propagate to and from each BLR channel on the experiment through circulators. Sensing interferometers typically use between 75%:25% and 90:10% splits, with most the power going through a collimating probe and illuminating the surface of interest because of the large return losses. The lower power leg propagates a path with a delay typically matched to the midrange of the surface travel. Figure 7 ignores polarization control and free space delay lines which may be added in each leg of the interferometer to adjust relative polarization and delay between target and reference signals. A filter is used to combine PDV measurement at shorter wavelength on the same probe as the BLR measurement. Fiber runs after the main sensing splitter will range from 30 to 200 m in length and be in ribbon cables because of the large numbers of diagnostics fielded in many experiments. Using the same ribbon for the signal and reference legs also helps minimize differential temperature variations which would be interpreted as target movement. Chromatic dispersion of the two legs must be balanced so fibers are sorted or chosen from the same spool to ensure good dispersion matches, and any filter needed in one leg is duplicated in the other simply to match dispersion profiles. PYISC modules typically use a 90%:10% splitter with short paths to high reflective mirrors to maintain stability.

3.3 Timing fiducial injection

Cross timing measurements vary from facility to facility and by the type of instrument. In BLR the biggest timing drifts are due to temperature changes of the 10s of km long dispersion and time delay single mode fibers. We are developing a timing fiducial injection system that will inject a < 1ns duration timing fiducial pulse on each channel at a known wavelength before any long dispersive fibers. This fiducial is driven by a trigger common to all channels and it marks a time point in the data that can be cross-timed independently of variations in the delay of the long fibers.

3.4 Back end multiplexing

We refer to the time domain multiplexing of multiple BLR channels on to one dispersive FT amplification system and one scope channel as back end multiplexing. Systems under development typically combine two BLR channels onto one scope channel simply by delaying one by more than the time period of interest and combining them with a high-speed optical switch. The diagram in Figure 7 shows a delay module made of SMF28 together with a DCM module zeroing out the chromatic dispersion of this delay as to not significantly change the distance to frequency calibration of the two channels being multiplexed. Dispersion compensation of the delay fiber is not required, but for typical system designs not doing so leads to a 10 to 25% reduction of the maximum range of delayed channels relative to the non-delayed channels.

4. CONCLUSION

We have discussed the history, physical concept of operation, non-idealities, and the multi-channel architecture R&D direction of BLR within the DOE national security labs. While there are differences in hardware under development due to schedules, component availability, facilities differences, and performance priorities, NSTec, LANL, and LLNL are collaborating on a common architectural approach and common analysis software[9]. We expect the final deployment instruments to be a blend of lessons learned and best practices from all the institutions.

ACKNOWLEDGEMENT

The authors would like to acknowledge the contributions of Matt Briggs, Jared Catenacci, Anselmo Garza, Steve Gilbertson, Patrick Harding, Susan Haynes, David Holtkamp, Marylesa Howard, Mandy Hutchins, Natalie Kostinski, Adam Lodes, Bruce Marshall, Kirk Miller, Reed Patterson, Mike Pena, Carlos Perez, Daniel Perry, George Rodriguez, Jose Sinibaldi, Vu Tran, Tony Whitworth, and many others. This work performed under the auspices of the U.S.

Department of Energy by Lawrence Livermore National Laboratory under Contract DE-AC52-07NA27344, by Los Alamos National Laboratory under Contract DE-AC52-06NA25396, and by National Security Technologies, LLC, under Contract DE-AC52-06NA25946.

REFERENCES

[1] Sargis, P. D., Molau, N. E., Sweider, D., Lowry M. E., and Strand, O. T., "Photonic doppler velocimetry," United States, doi:10.2172/8025, (1999).

[2] Strand, O. T., and Whitworth T. L., "Using the heterodyne method to measure velocities on shock physics experiments," AIP Conference Proceedings **955**, 1143 (2007).

[3] Briggs, M., et al, "Optical distance measurements to recover the material approach missed by optical velocimetry," J. Phys.: Conf. Ser. **500**, 142005 (2014).

[4] Xia, H. and Zhang, C., "Ultrafast ranging lidar based on real-time Fourier transform," Opt. Lett., **34**, 14, (2009).

[5] Xia, H. and Zhang, C. "Ultrafast and Doppler-free femtosecond optical ranging based on dispersive frequency-modulated interferometry," Opt. Express **18**, 4118-4129 (2010).

[6] La Lone, B. M., Marshall, B. R., Miller, E. K., Stevens, G. D., Turley, W. D., and Veeser, L. R., "Simultaneous broadband laser ranging and photonic Doppler velocimetry for dynamic compression experiments," Rev. Sci. Inst. **86**, 023112 (2015).

[7] La Lone, B. M., Marshall, B., Bennett, C., Miller, K., Stevens, G., Turley, W., Younk, P., and Briggs, M. "Simultaneous broadband laser ranging and PDV," 19th Biennial Conference of the APS Topical Group on Shock Compression of Condensed Matter **60**, 8, Tampa, Florida, June 14–19, (2015).

[8] Chou, J., Solli, D. R., and Jalali, B., "Real-time spectroscopy with subgigahertz resolution using amplified dispersive Fourier transformation," Appl. Phys. Lett. 92(11), 1111021–1111023 (2008).

[9] Kostinski N., Rhodes, M. A., Catenacci J., Howard M, La Lone, B. M., Bennett, C. V., Harding, P. J., "Broadband laser ranging: Signal analysis and interpretation," Proc. SPIE 10089, **15**, (2017).

[10] Hamp, M. J., Wright, J., Hubbard, M. and Brimacombe, B., "Investigation into the temperature dependence of chromatic dispersion in optical fiber," IEEE Photon. Tech Lett., **14**, 11, (2002).